5th International Conference on Experimental Fluid Mechanics ICEFM 2018 Munich
Munich, Germany, July 2-4, 2018

Three-dimensional bluff body flow: bridging instantaneous and averaged flow structures with highly pulsatile flow

Ian A. Carr, Nikolaos Beratlis, Elias Balaras, Michael W. Plesniak*

The George Washington University, Department of Mechanical & Aerospace Engineering, Washington, DC, USA

*plesniak@gwu.edu

Abstract

The instantaneous flow field in the wake of a surface-mounted hemisphere exposed to a highly pulsatile freestream was investigated using experiments and direct numerical simulations. The simulations accompany a set of experiments performed under the same conditions using phase-averaged planar particle image velocimetry. The wake of the hemisphere during the acceleration phase has been visualized with streamlines and iso-surfaces of pressure through acceleration. The acceleration phase has been compared with wakes resulting from a constant velocity freestream (steady flow) at similar Reynolds numbers. A relationship between a starting vortex and the arch vortex in the recirculation zone has been proposed. The instantaneous flow fields elucidate the existence and formation of the arch vortex as an instantaneous structure rather than an artifact of averaging.

1 Introduction & Background

Canonical flows around surface-mounted bluff bodies have a wide range of applications. Bluff body geometries like hemispheres serve as an abstractions for more complex natural and engineering bodies. While fairly simple, these geometries produce complex fluid dynamics making them attractive for simulation benchmarking purposes. The classical primary flow structures produced by a surface-mounted hemisphere are the horseshoe or necklace vortex formed at the windward junction, and hairpin vortices shed downstream periodically.(Acarlar and Smith, 1987) Alternate descriptions of the flow, often based on time-averaged data, depict stationary arch-shaped vortex structures in the near wake or recirculation zone. (Manhart, 1998; Savory and Toy, 1986) Both of these representations are accepted and valid, but what is missing is the link between the two representations? Are the instantaneous and time-averaged depictions of the wake independent or connected? Our studies of highly pulsatile flow have shown themselves to be helpful in understanding the connection.

Figure 1 consists of a series of wake representations from previous studies (Tamai et al., 1987; Manhart, 1998; Savory and Toy, 1986). Figure 1a is a canonical representation of the instantaneous flow structures, notably the classical hairpin vortices in the wake. Figures 1b and 1c are similar representations of averaged flow structures. While the primary wake structures in Figure 1a are the hairpin vortices and the primary structure in Figure 1b and 1c is the arch-shaped recirculation vortex. Neither of these representations is complete and do not fully represent the wake. The existence of the arch vortex is still a debated topic. (Johnson et al., 2017) A full understanding and representation of the wake structures should include structures from both. Instantaneous and averaged structures operate of different timescales, form, and influence their surroundings differently.

Addressing the discrepancies in wake structures was not the original goal of our studies concerning pulsatility, but the cyclic nature of pulsatility has proven to be a useful tool in understanding bluff body wakes more generally. A flow is considered highly pulsatile when the amplitude of the cyclic fluctuations is on the same order as the mean flow and the period of the fluctuations is sufficiently short, i.e. the acceleration and deceleration phases are severe enough to not produce a set of quasi-steady results. Figure 2 is an example of three highly pulsatile flows. The black profile is the one investigated in this study. It is convenient to separate the inflow waveform into two primary segments, acceleration and deceleration. Acceleration

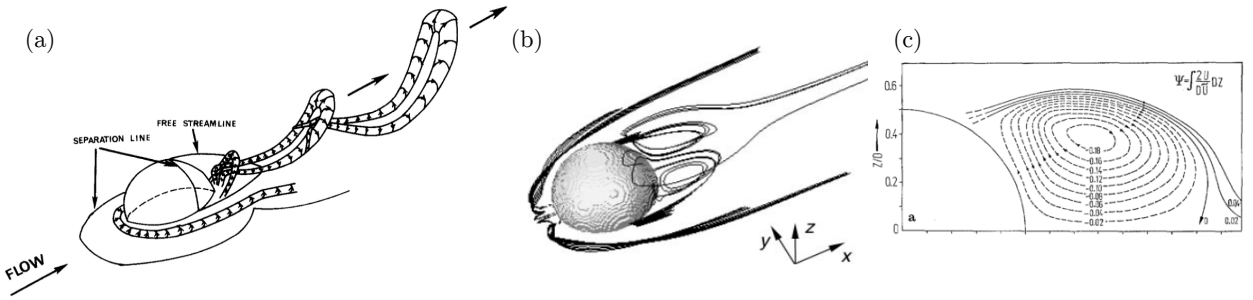

Figure 1: (a) Schematic representation of the instantaneous flow structures around a hemisphere (Tamai et al., 1987), (b) Computed averaged streamlines in the near wake of a hemisphere results (Manhart, 1998), (c) Depiction of a vertical slice of the averaged streamlines in the near wake of a hemisphere (Savory and Toy, 1986).

provides a view into the formation of the wake and deceleration highlights the behavior of the wake when not influenced by the freestream. When carefully observed, the two segments can emphasize and elucidate dynamics that are not obvious in steady flow.

It is common practice in the study of vortex dynamics to investigate the formation of a vortex to learn about its nature. In typical studies of bluff body flow the measurements are taken after the flow has reached a steady freestream velocity giving no opportunity to observe the formation some wake structures. For structures like the hairpin vortices, which form and shed cyclically from the shear layer, steady flow allows the experimenter to see their formation. For a structure like the arch vortex in the recirculation region a view of its initial formation cannot be attained directly with a steady freestream. If viewed in pulsatile flow the one can observe the arch vortex formation with every acceleration phase.

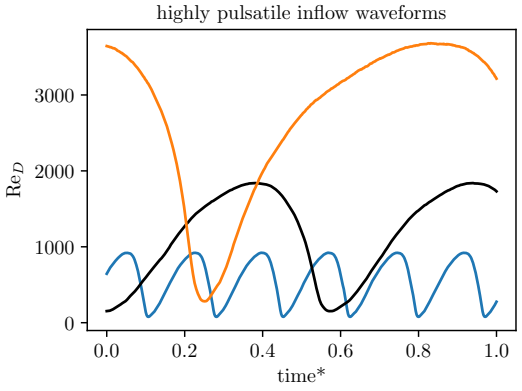

Figure 2: Examples of highly pulsatile flow profiles

2 Methods

2.1 Numerical Methods

The pulsatile simulations are carried out using an in-house finite difference Navier-Stokes code. The governing equations for a viscous incompressible flow are discretized on a structured grid in Cartesian space. The geometry of the hemisphere, which is not aligned with the grid, is treated using an immersed-boundary formulation. An exact, semi-implicit projection method is used for time advancement. All terms are treated explicitly using a Runge-Kutta 3rd order scheme with the exception of the viscous and convective terms in the wall-normal direction. Those terms are treated implicitly using a 2nd order Crank-Nicholson scheme. All spatial derivatives are discretized using a 2nd order, central-difference scheme on a staggered grid. The code is parallelized using a classical domain decomposition approach. The domain is evenly divided in the streamwise direction and communication between the processed is handed with MPI library calls. The inlet boundary condition is a uniform pulsatile velocity matched with the experiments. More details of the solver can be found in Beratlis et al. 2007.

2.2 Experimental Methods & Numerical Validation

A series of experiments has led to the simulation results being presented herein. Those experiments were performed in a suction-based, low-speed wind tunnel equipped with a set of rotating vanes at the test sections exit. These rotating vanes vary the blockage ratio from 20% when aligned with the direction of flow to 99%

when perpendicular to the direction of flow creating a pulsatile inflow waveform similar to that in Figure 2. A TSI planar particle image velocimetry (PIV) system was used for measurements of the wake and incoming boundary layer. The PIV capture system was synchronized with the motion of the rotating vanes to facilitate phase-averaging. The inflow profile was broken into 36 phases and 100 image pairs were captured at each phase. Additionally, a Dantech MiniCTA hotwire anemometer was used for highly resolved (in time) point measurements of the pulsatile profile and frequency content in the wake. The incoming boundary layer thickness is approximate half one obstacle height ($\delta/h = 0.5$). For more information on the experimental setup refer to our previous publications. (Carr and Plesniak, 2016, 2017)

The simulations were validated against the experiments in two ways: by comparing a set of streamwise velocity profiles upstream of the obstacle and in the obstacle's wake and correlating of a two dimensional plane of data in the close proximity of the obstacle. The data was a 93% match between simulation and experimental velocity magnitude averaged over the the cycle, with the lowest overall correlation being 87%. Additionally the relevant flow physics were captured and are nearly indistinguishable from experiment.

3 Results & Discussion

The near wake of a surface-mounted hemisphere in a pulsatile freestream will be discussed. Specifically, we will describe the formation of the arch vortex throughout the acceleration segment of the pulsatile inflow waveform and explain how it relates to the steady state case. A relationship based on the formation of a starting vortex and the steady state recirculation bubble will be proposed.

3.1 Pulsatile Freestream

To observe the formation and growth of the arch vortex and recirculation zone, four instantaneous realizations during the acceleration segment were investigated. The distinct points during the acceleration segment of a pulsatile waveform are shown in Figure 3 with red dots. The waveform has a mean Reynolds number based on diameter D, Re_m, of 1290, a total Re variation of 2000, and a non-dimensional frequency of 0.054 (fD/U where f is the frequency of the large scale oscillation and U is time-average freestream velocity in the x-direction). The wake of the hemisphere during acceleration is shown in Figure 4. The streamlines are seeded randomly in a shell of diameter 1.1 D surrounding the hemisphere. The pressure contour thresholds were set at each phase to best emphasize the wake. A single pressure threshold cannot be used in pulsatile flow due to the large pressure fluctuations during the inflow cycle.

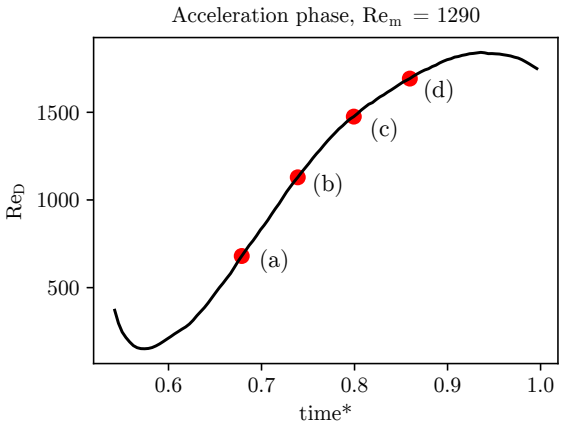

Figure 3: Phases corresponding to the pressure contours in Figure 4.

The stages of development of the arch vortex and near wake are typified by the four realizations in Figure 4. Figure 4a shows the flow shortly after the boundary layer on the hemisphere separates and the arch vortex begins to form. In the case of the hemisphere the recirculation zone and arch vortex are one in the same. In Figure 4b the arch vortex has grown and gained clarity and coherence. Circular stream lines clearly mark an arch shaped structure and the low pressure contour clearly forms in the center of the curved streamlines. In Figure 4c the arch vortex expands further downstream along with the low pressure region and reattachment. And finally in Figure 4d the wake turbulence increases to the point arch vortex organization begins to lose coherence and the pressure contour becomes less defined.

Figure 4 also shows surface pressure contours. The surface pressure contours identify critical points on the surface i.e. approximate point of separation, the presence of a near surface vortex, a recirculation region, etc. In Figure 4 the "B" shaped imprint of the recirculation zone can be observed in all four phases. Additionally, an approximate line of boundary layer separation can be seen as an abrupt transition from high surface pressure (red) to low surface pressure (blue). In all realizations this region shows a decreased

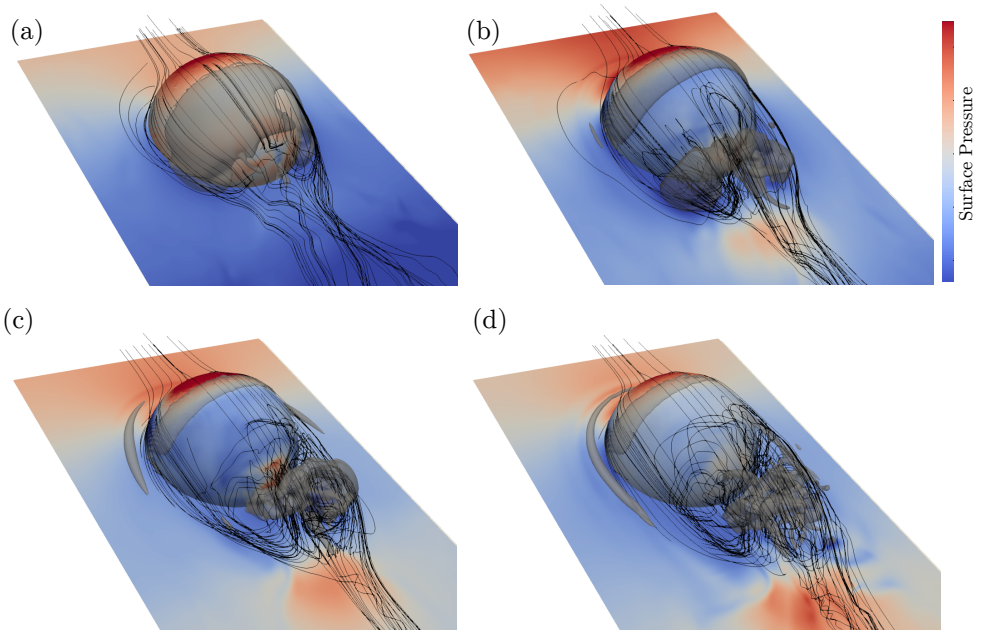

Figure 4: Iso-surfaces of pressure in grey and contours of surface pressure on ground plane and obstacle surface. The phase of each visualization is in Figure 3

pressure near the same magnitudes as in the wake. The pressure iso-surfaces provide a compelling case for the an arch shaped vortex in the acceleration phase.

Throughout the acceleration segment of the pulsatile waveform it's clear that the arch vortex clearly exists, as viewed through circular streamlines or contours of pressure. In pulsatile flow it is clearly not only a flow structure in an averaged sense, but in an instantaneous sense as well.

3.2 Steady Freestream

Figure 5 shows iso-surfaces of pressure and streamlines at Re near the minimum and maximum values observed in the pulsatile case. The Reynolds number ranges between Re = 645 and Re = 2580. The streamlines and pressure contours were produced using the same techniques as in Figure 4. The pressure iso-surfaces in steady flow are spatially stationary but are located further downstream and further from the wall. The pocket of low pressure is not in the near wake as it was in the pulsatile case. Instead it is in the area near the curved free shear layer where the hairpins shed. In Figure 5a a portion of one of the hairpins is visible roughly 3D downstream of the hemisphere.

The arch-like organization is highlighted by the streamlines in both Figures 5a and b, though the organization is clearer in the the lower Re, Figure 5a, case as the wake is less turbulent; an intuitive result. In both wake representations there is evidence for an arch-type structure in the wake, but with lessorganization and different morphology than the pulsatile case.

3.3 The starting vortex

In this section we will attempt to explain why the arch vortex is differs in steady flow compared to the pulsatile case using starting vortices as a basis for understanding. A starting vortex is a vortex formed as a result of accelerating a body from rest through a fluid. The most commonly studied scenario for starting vortices is an airfoil accelerated through a quiescent field. (Chang et al., 1993; Agromayor and Kristoffersen, 2014; Auerbach, 1987) There have been some studies of starting vortices in the wake of two dimensional ribs, and some bluff bodies. (Molochnikov et al., 2017; Pullin and Perry, 1980; Lian and Huang) Specifically the study by Lian et al. (1989) of starting vortices produced with flat plates oriented normal to the flow provides insight into the organization (or lack thereof) in the wake of a hemisphere.

We propose that a starting vortex forms in the wake of the hemisphere with each acceleration phase. Due to the frequency of the inflow waveform this vortex cannot fully form. Instead, quickly after it forms the

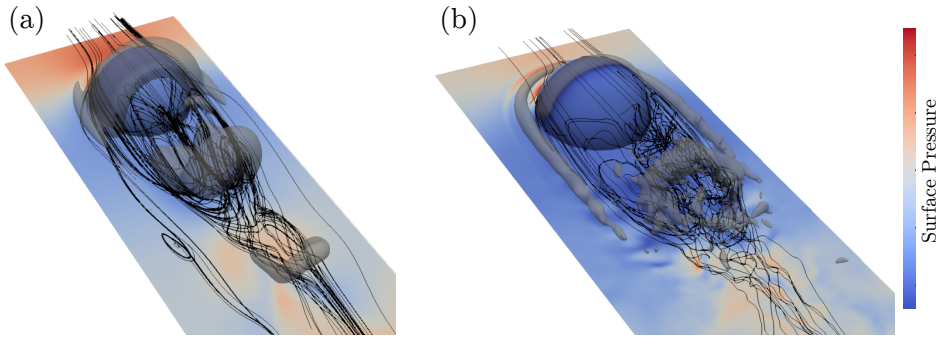

Figure 5: Steady flow around a surface mounted-hemisphere. Visualization with streamlines, surface pressure contours and iso-surfaces of pressure at (a) Re = 645 and (b) Re = 2580

deceleration phase occurs and the vortex propagates upstream, and is shed into the wake in the accelerating flow as discussed in detail in our previous publications (Carr and Plesniak, 2016, 2017).

The starting vortex and steady state recirculation zone/arch vortex share the same sense of rotation, approximate position, and morphology. The primary difference is the degree of instantaneous coherence in the starting vortex and the lack thereof in the arch vortex. When averaged (phase-averaged in the pulsatile case and ensemble-averaged in steady case) the two structures appear to be one in the same. At the Re range and frequency of pulsatility observed in the pulsatile case the hairpin vortices are not formed because the shear layer has not reach a steady state. Once that steady state is reached the hairpin structures begin to form and become the most prominent structure in the flow. The progression from starting vortex through some transition to vortices shed cyclicly from the shear layer which surrounds a rotating recirculation zone is commonplace in the study of starting wakes. The understanding that a surface-mounted hemisphere follows the same progression as an airfoil, fence, disc, etc., allows for the knowledge gained in those previous studies to be applied to a wider range of geometries. The starting vortex of low aspect ratio, surface-mounted obstacle has not previously been reported.

4 Future experiments

Starting vortices have been observed in numerous instances in nature, e.g. certain modes of flapping flight is one of the most notable. In these numerous occurrences there are numerous applications. Starting vortices around surface-mounted bluff bodies have not before been documented in pulsatile flow, and perhaps not even in steady flow. Possible control of starting vortices in the wake of surface-mounted bluff bodies could be useful in many engineering applications.

A series of experiments using geometry to control, enhance, or weaken the starting vortices would be interesting and enlightening. Instantaneous and phase-averaged fields are necessary to fully understand the wakes. Performing high fidelity phase-averaged simulations requires computation times that are orders of magnitude longer than similar experiments would take, therefore using a combination of phase-averaged and time-resolved experiments appears most practical. A series of experiments aimed at understanding the starting vortex and its behavior through the deceleration segment focused on control through geometry and surface roughness will be performed using time-resolved, planar PIV in our recently completed small-scale pulsatile wind tunnel. Fine adjustment of the pulsatile inflow waveform possible in updated experiment will allow for a greater range of amplitudes, frequencies, offsets, and inflow profile shapes greatly expanding the possible applications impacted by future studies.

5 Conclusion

The wake of a surface mounted hemisphere subjected to a highly pulsatile freestream has been investigated using a combination of experiments and simulations. The results from the instantaneous results from a pulsatile and steady freestream simulations have been presented. The arch vortex, observed in the steady case often through averaging, has been compared with the starting vortex in the pulsatile case. The starting vortex has a greater degree of organization at the same Re than the arch vortex in the steady case which agrees with

previous literature on starting vortices and the steady state case that follows. This study extends the application of knowledge gained from the study of starting vortices to low aspect ratio, surface-mounted bluff bodies. A series of experiments on starting vortex control has been proposed. The proposed experiments would be performed in a recently competed small-scale pulsatile wind tunnel which enables experimentation on numerous geometries at rate not possible with simulations.

Acknowledgements

The Center for Biomemetic and Bio-inspired Engineering (COBRE) at George Washington University

References

AbuOmar MM and Martinuzzi RJ (2008) Vortical structures around a surface-mounted pyramid in a thin boundary layer. *Journal of Wind Engineering and Industrial Aerodynamics* 96:769–778

Acarlar MS and Smith CR (1987) A study of hairpin vortices in a laminar boundary layer. Part 2. Hairpin vortices generated by fluid injection. *Journal of Fluid Mechanics* 175:43

Agromayor R and Kristoffersen R (2014) Simulation of Starting and Stopping Vortices of an Airfoil. in *Proceedings of the 58th SIMS*. pages 66–75

Auerbach D (1987) Experiments on the trajectory and circulation of the starting vortex. *Journal of Fluid Mechanics* 183:185–198

Carr IA and Plesniak MW (2016) Three-dimensional flow separation over a surface-mounted hemisphere in pulsatile flow. *Experiments in Fluids* 57:1–9

Carr IA and Plesniak MW (2017) Surface obstacles in pulsatile flow. *Experiments in Fluids* 58:152

Chang C, Hsiau Y, and Chu C (1993) Starting vortex and lift on an airfoil. *Physics of Fluids A: Fluid Dynamics* 5:2826–2830

Haller G (2005) An objective definition of a vortex. *Journal of Fluid Mechanics* 525:1–26

Hunt JCR, Wray AA, and Moin P (1988) Eddies, streams, and convergence zones in turbulent flows. in *Studying Turbulence Using Numerical Simulation Databases, 2. Proceedings of the 1988 Summer Program*. volume 1. pages 193–208

Johnson KC, Thurow BS, Kim T, Blois G, and Christensen KT (2017) Volumetric Velocity Measurements in the Wake of a Hemispherical Roughness Element. *AIAA Journal* 55:1–16

Lian QX and Huang Z () Starting flow and structures of the starting vortex behind bluff bodies with sharp edges. *Experiments in Fluids* 8:95–103

Manhart M (1998) Vortex Shedding from a Hemisphere in a Turbulent Boundary Layer. *Theoretical and Computational Fluid Dynamics* 12:1–28

Molochnikov V, Kalinin I, Mazo B, Malyukov V, Okhotnikov DI, and Dushina OA (2017) Vortex shedding behind an obstacle in a channel under transition to turbulence in steady and pulsating flows. *IOP Conf Series: Journal of Physics: Conf Series* 899

Pullin DI and Perry AE (1980) Some flow visualization experiments on the starting vortex. *Journal of Fluid Mechanics* 97:239–255

Savory E and Toy N (1986) The flow regime in the turbulent near wake of a hemisphere. *Experiments in fluids* 188:181–188

Stewart KC, Erath BD, and Plesniak MW (2013) Investigating the Three-Dimensional Flow Separation Induced by a Model Vocal Fold Polyp. *Journal of Visualized Experiments*

Tamai N, Asaeda T, and Tanaka N (1987) Vortex structures around a hemispheric hump. *Boundary-layer meteorology* 39:301–314